Detailed reaction mechanism of *n*-butane oxidation

Frolov S. M.[1], Basevich V. Ya.[1], Belyaev A. A.[1], Pasman H. J.[2]
[1]Semenov Institute of Chemical Physics, Moscow, Russia, smfrol@chph.ras.ru
[2]Delft University of Technology, Delft, The Netherlands

Abstract

Detailed reaction mechanisms of hydrocarbon oxidation contain hundreds species and thousands reactions and incorporate multiple intermediate molecules, isomers, and radicals. Despite many fundamental advantages inherent in such mechanisms, their use in applied studies of combustion and explosion dynamics is impossible nowadays due to their complexity. In addition, these mechanisms cannot be considered as comprehensive as their applicability is usually limited by certain constraints. This paper is an attempt to use an automated algorithm for developing an optimal rather than "maximal" reaction mechanism aimed at correct description of main elementary processes governing the overall reaction rate and formation of principal intermediate and final products. Such a mechanism has a status of nonempirical detailed reaction mechanism as its elementary reactions are fundamentally substantiated. The mechanism has two specific features: (1) it does not include reactions of double oxygen attachment (first to a peroxide radical and then to its isomer), i.e., the first attachment is assumed to be sufficient; and (2) reactions with isomer compounds and their derivatives are not considered because the corresponding oxidation routes are slower than the routes via molecules and radicals of normal structure. The use of the algorithm allows the development of relatively compact oxidation mechanisms for heavy *n*-alkanes. In this paper, such a mechanism has been developed and validated for *n*-butane.

Introduction

Detailed reaction mechanisms of hydrocarbon oxidation contain hundreds species and thousands reactions and incorporate multiple intermediate molecules, isomers, and radicals. For example, the detailed mechanisms of *n*-heptane and *n*-decane oxidation contain 650 species and 2300 reactions [1], and 715 species and 3872 reactions [2], respectively. Despite many fundamental advantages inherent in such mechanisms, their use in applied studies of oxidation, combustion, and explosion dynamics is impossible nowadays due to their complexity. In addition, these mechanisms cannot be considered as comprehensive as their applicability is usually limited by certain constraints. Simple estimations indicate that the account for all possible isomers and reactions between all species involved would result in much more complex detailed reaction mechanisms than those in [1, 2]. For example, if one includes reactions of PAH, soot, and fullerenes formation and consumption, the reaction mechanisms would likely contain tens of thousands reactions. The other problem associated with the development of such detailed reaction mechanisms is the absence of reliable data on thermochemical parameters and reaction rate constants for many relevant species and reactions. This issue is important indeed for estimating the accuracy and predicting capability of such mechanisms.

As a matter of fact, for most applications there is often a need in optimal rather than "maximal" reaction mechanisms. The optimal reaction mechanism implies that it contains main elementary stages determining the overall rate of the oxidation process as well as main intermediate and final reaction products. Such optimal mechanisms, even if they are sufficiently compact, will have a status of nonempirical reaction mechanisms once they are composed of elementary reactions with kinetically substantiated reaction rate constants.

Thus, there is a nonextensive way of constructing reaction mechanisms of hydrocarbon oxidation and combustion. Such mechanisms, despite certain limitations in representing possible reactions and species, still preserve the main routes of chemical transformation and principal types of elementary reactions. Such mechanisms can be constructed using an automated algorithm.

Phenomenology of *n*-alkane oxidation is known to be quite general [3, 4]. In this paper, we developed the algorithm aimed at constructing the oxidation mechanism of *n*-alkanes and applied it for *n*-butane, C_4H_{10}. The oxidation mechanisms of C_4H_{10} have been already reported elsewhere [5, 6]. Contrary to [5, 6], the mechanism developed in this paper is relatively compact and is based on the following main assumptions [7]: (1) low-temperature chain branching is assumed to be governed by the group of elementary reactions with one oxygen attachment, and (2) the oxidation route via the isomers can be neglected as it is slower than the oxidation route via the compounds of normal structure (i.e., we do not make difference between the species of normal and isomer structure).

One can expect that such an approach will result in a nonempirical detailed reaction mechanism for modeling *n*-alkane oxidation and combustion. This mechanism will not be comprehensive and will not provide complete composition of intermediate and final products in the reaction zone, but will be more compact and still informative. The latter is important in particular for construction of oxidation mechanisms for high *n*-alkanes, C_nH_{2n+2}.

1. Algorithm

To develop the kinetic mechanism based on the assumptions adopted above, a special mathematical procedure has been developed. In the procedure, the mechanism of the lower *n*-alkane analog in the homological series with n - 1 carbon atoms is taken as a basis for the oxidation mechanism of C_nH_{2n+2} hydrocarbon. This relates both to species and to reactions.

Let us consider the use of this principle for *n*-butane. For *n*-butane, the lower analog in the homological series is propane. Therefore the mechanism of propane oxidation and combustion can be taken as a basis for constructing the corresponding mechanism for *n*-butane. The propane oxidation mechanism has been developed earlier [7]. It includes 45 species and 204 reversible reactions and describes satisfactorily both low-temperature and high-temperature oxidation and combustion of methane, ethane, and propane. Following the principle adopted, the oxidation mechanism of C_4H_{10} was composed from the oxidation mechanism of C_1-C_3 hydrocarbons and supplementary species and reactions analogous to the species and reactions present in the C_1-C_3 mechanism. In addition, supplementary reactions between hydrocarbon radicals and molecules relevant to C_4H_{10} have to be included into the mechanism. Thus, in the oxidation mechanism of *n*-butane, the analogs for radicals C_3H_7, C_3H_7O, and $C_3H_7O_2$ from the propane oxidation mechanism are radicals C_4H_9, C_4H_9O, and $C_4H_9O_2$, and so on. The list of new species in the *n*-butane oxidation mechanism, which are similar to those in the propane oxidation mechanism, is presented in Table 1. Also shown in Table 1 are the formation enthalpies ΔH^o_{f298} and entropies S_{298}, taken from textbooks or calculated by the additive technique.

The same relates to reactions. For example, the analogs of reactions $C_3H_7 + O_2 = C_3H_7O_2$, $C_3H_8 + OH = C_3H_7 + H_2O$, and $C_3H_8 = C_3H_7 + H$ in the propane mechanism are the following reactions in the oxidation mechanism of *n*-butane: $C_4H_9 + O_2 = C_4H_9O_2$, $C_4H_{10} + OH = C_4H_9 + H_2O$, and $C_4H_{10} = C_4H_9 + H$, and so on. Moreover, the oxidation mechanism of *n*-butane has to be extended: instead of two monomolecular reactions $C_3H_8 = C_3H_7 + H$ and $C_3H_8 = C_2H_5 + CH_3$ in the propane mechanism, the oxidation mechanism of *n*-butane will contain three reactions: $C_4H_{10} = C_4H_9 + H$, $C_4H_{10} = C_3H_7 + CH_3$ and $C_4H_{10} = C_2H_5 + C_2H_5$, and so on.

One of the most important issues for the detailed mechanism is the choice of Arrhenius parameters for the reaction rate constants. Unfortunately, reliable information on the reaction rate constants is available only for a limited number of elementary reactions and is absent even for the most important rate-limiting reactions for hydrocarbons. Therefore assuming that the reaction rate constants in the known oxidation mechanism of propane are reasonable, one can use this information for estimating the corresponding rate constants in the oxidation mechanism of *n*-butane.

A two-parameter rate constant for the *i*th reaction is defined as:

$$k_i = A_i \exp(-E_i / RT)$$

Table 1: Additional species in the oxidation mechanism of *n*-butane

No.	Species	ΔH^o_{f298} kcal/mole	S_{298} cal/mole/K
46	C_4H_{10}	-29.6	64.51
47	C_4H_9	18.46	77.34
48	$C_4H_9O_2$	-10.5	101.38
49	$C_4H_9O_2H$	-40.6	93.3
50	C_4H_9O	-6.5	86.1
51	C_3H_7CHO	-50.7	82.2
52	C_3H_7CO	-16.0	83.5
53	C_4H_8	-2.74	73.52
54	C_4H_7	26.36	70.1

where A_i is the preexponential factor, E_i is the activation energy, T is the temperature, and R is the gas constant. The preexponential factor A_i is known to be proportional to $\exp(\Delta S_i/R)$, where ΔS_i is the variation of the reaction entropy. For the reactions of the same type (see above) in the oxidation mechanisms of C_nH_{2n+2} hydrocarbon and propane (n = 3), the following relationship is valid:

$$A_{i\,(n)}=A_{i(n=3)}\exp[(\Delta S_{i(n)}-\Delta S_{i(n=3)})/R]$$

For the activation energy $Å_i$, the following approximate rule is known [8]:

$$E_i=11.5-0.25\Delta H_i \text{ for exothermic reactions, and}$$
$$E_i=11.5+0.75\Delta H_i \text{ for endothermic reactions}$$

where ΔH_i is the variation of reaction enthalpy. Therefore for the reactions of the same type in the oxidation mechanisms of C_nH_{2n+2} hydrocarbon and propane (n = 3), the following approximate correlations are valid:

$$E_{i(n)}=E_{i(n=3)}-0.25[\Delta H_{i(n)}-\Delta H_{i(n=3)}] \text{ for exothermic reactions, and}$$
$$E_{i(n)}=E_{i(n=3)}+0.75[\Delta H_{i(n)}-\Delta H_{i(n=3)}] \text{ for endothermic reactions}$$

where $\Delta H_{i(n)}$ and $\Delta H_{i(n=3)}$ are the corresponding variations of reaction enthalpy. Thus, one can use the values of Arrhenius parameters of the reaction rate constant from the propane mechanism for estimating the corresponding reaction rate in the oxidation mechanism of hydrocarbon with $n > 3$, including *n*-butane. Based on such estimations, the algorithm and computer code for constructing the oxidation mechanism of *n*-alkanes have been developed. In particular, the oxidation mechanism of *n*-butane thus obtained included 9 additional species (Table 1) and 84 additional elementary reactions (Table 2) as compared to the propane oxidation mechanism. The complete number of species and reactions in the *n*-butane mechanism is 54 and 288, respectively. In addition to the estimates of Arrhenius parameters discussed above, all available literature data on the reaction rate constants were used.

It is well known that various critical phenomena like the onset of cool and blue flames at multistage self-ignition are very sensitive to the values of reaction rate constants and manifest themselves at a proper relationship between the rates of different elementary stages. Therefore, one can fail to model the phenomena observed in practice without additional correction of reaction rate constants of some important elementary stages. In view of it, an additional correction of the reaction rate constants within the experimental uncertainty and within the ranges allowed by the kinetic theory could be required. For the *n*-butane oxidation mechanism, such a correction procedure was required for 8 reactions including the reactions of *n*-butane with hydroperoxide radicals and reactions of butyl radical with molecular oxygen.

Table 2: Mechanism of *n*-butane oxidation

No.	Reaction	*A* mole, l, s	*E/R* K
1	C4H10 + O2 = C4H9 + HO2	0.259E+10	0.240E+05
2	C4H10 + OH = C4H9 + H2O	0.409E+10	0.580E+03
3	C4H10 + H = C4H9 + H2	0.603E+11	0.401E+04
4	C4H10 + O = C4H9 + OH	0.328E+12	0.481E+04
5	C4H10 + HO2 = C4H9 + H2O2	0.389E+09	0.862E+04
6	C4H8 + H = C4H9	0.141E+10	0.652E+03
7	C4H9 + O2 = C4H8 + HO2	0.300E+11	0.700E+04
8	C4H9 + OH = C4H8 + H2O	0.803E+10	-0.337E+03
9	C4H10 = H + C4H9	0.233E+14	0.376E+05
10	C4H10 = CH3 + C3H7	0.324E+16	0.422E+05
11	C4H10 = C2H5 + C2H5	0.194E+17	0.428E+05
12	C4H9 + H = C4H8 + H2	0.803E+10	-0.337E+03
13	C4H9 + CH3 = C4H8 + CH4	0.470E+09	-0.443E+03
14	C4H9 + C2H5 = C4H8 + C2H6	0.131E+09	0.128E+03
15	C4H9 + C3H7 = C4H8 + C3H8	0.184E+09	0.151E+03
16	C4H9 + O = C4H8 + OH	0.268E+12	-0.337E+03
17	C4H9 + O2 = C4H9O2	0.684E+09	-0.659E+03
18	C4H10 + CH3O2 = C4H9 + CH3O2H	0.890E+10	0.600E+04
19	C4H10 + C2H5O2 = C4H9 + C2H5O2H	0.890E+10	0.600E+04
20	C4H10 + C3H7O2 = C4H9 + C3H7O2H	0.890E+10	0.600E+04
21	C4H10 + C4H9O2 = C4H9 + C4H9O2H	0.890E+10	0.600E+04
22	C4H9O2H = C4H9O + OH	0.643E+16	0.198E+05
23	C4H9O = H2CO + C3H7	0.257E+15	0.983E+04
24	C4H9O = CH3CHO + C2H5	0.627E+15	0.975E+04
25	C4H9O = C2H5CHO+ CH3	0.126E+15	0.991E+04
26	C4H9O = C4H8O + H	0.108E+13	0.834E+04
27	C4H9O2+ H = C4H9O + OH	0.105E+10	-0.830E+03
28	C4H9O2+ CH3 = C4H9O + CH3O	0.162E+08	0.614E+03
29	C4H9O2+ C2H5 = C4H9O + C2H5O	0.369E+08	0.131E+03
30	C4H9O2+ C3H7 = C4H9O + C3H7O	0.281E+08	0.780E+03
31	C4H9O2+ C4H9 = C4H9O + C4H9O	0.214E+08	0.140E+04
32	C4H9O2+ H2CO = C4H10O2+ HCO	0.111E+08	0.353E+04
33	C4H9O2 + CH3CHO = C4H10O2+ CH3CO	0.109E+08	0.364E+04
34	C4H9O2 + C2H5CHO = C4H10O2 + C2H5CO	0.109E+08	0.382E+04
35	C4H9O2 + C4H8O = C4H10O2 + C4H7O	0.109E+08	0.401E+04
36	C4H9 + HO2 = C4H9O + OH	0.229E+11	0.622E+03
37	C4H9 + O2 = C4H8O + OH	0.479E+10	0.893E+04
38	C4H9 + C2H5 = C4H10 + C2H4	0.963E+09	0.355E+03
39	C4H9 + C3H7 = C4H10 + C3H6	0.293E+10	0.201E+02
40	C4H9 + C4H9 = C4H10 + C4H8	0.392E+10	-0.317E+03
41	C4H9 + O2 = H2CO + C3H7O	0.400E+09	0.500E+04
42	C4H9 + O2 = CH3CHO + C2H5O	0.400E+09	0.500E+04
43	C4H9 + O2 = C2H5CHO + CH3O	0.400E+09	0.500E+04
44	C4H9 + OH = CH3 + C3H7O	0.229E+11	-0.194E+04
45	C4H9 + OH = C2H5 + C2H5O	0.179E+12	-0.228E+03
46	C4H9 + OH = C3H7 + CH3O	0.132E+11	0.481E+03
47	C4H9 + H = CH3 + C3H7	0.480E+11	0.547E+03

48	C4H9 + H = C2H5 + C2H5	0.287E+12	0.322E+03
49	C4H9 + H = CH2 + C3H8	0.845E+10	0.302E+04
50	C4H9 + H = C2H4 + C2H6	0.127E+10	-0.643E+04
51	C4H9 + H = C3H6 + CH4	0.232E+10	-0.711E+04
52	C4H9 + O = H + C4H8O	0.842E+09	0.494E+03
53	C4H9 + O = CH3 + C2H5CHO	0.979E+11	-0.951E+03
54	C4H9 + O = C2H5 + CH3CHO	0.487E+12	-0.111E+04
55	C4H9 + O = C3H7 + H2CO	0.200E+12	-0.252E+01
56	C4H7O + HO2 = C4H8O + O2	0.530E+08	0.629E+02
57	C4H8O + OH = C4H7O + H2O	0.100E+11	-0.629E+02
58	C4H8O + H = C4H7O + H2	0.140E+11	0.159E+04
59	C4H8O + O = C4H7O + OH	0.568E+10	0.717E+03
60	C4H8O + HO2 = C4H7O + H2O2	0.600E+09	0.494E+04
61	C3H7 + HCO = C4H8O	0.216E+11	-0.679E+02
62	C3H7 + CO = C4H7O	0.181E+09	0.229E+04
63	C4H7O + H = C3H7 + HCO	0.501E+10	0.253E+04
64	C4H7O + O = C3H7O + CO	0.381E+10	0.780E+03
65	C4H8 + OH = C4H7 + H2O	0.241E+11	0.392E+04
66	C4H7 + H2 = C4H8 + H	0.319E+12	0.735E+04
67	C4H7 + O2 = C2H5O2 + C2H2	0.608E+11	0.547E+04
68	C4H8 + HCO = C4H7 + H2CO	0.161E+11	0.698E+04
69	C4H8 + CH3 = C4H7 + CH4	0.286E+08	0.336E+04
70	C4H8 + C2H5 = C4H7 + C2H6	0.797E+07	-0.105E+04
71	C4H8 + C3H7 = C4H7 + C3H8	0.112E+08	-0.112E+04
72	C2H5 + C2H2 = C4H7	0.330E+09	0.176E+04
73	C4H8 = C2H3 + C2H5	0.446E+14	0.369E+05
74	C4H8 = C3H5 + CH3	0.268E+13	0.429E+05
75	C4H8 + O2 = C4H7 + HO2	0.161E+11	0.215E+05
76	C4H8 + O = C3H7 + HCO	0.373E+10	0.565E+03
77	C4H7 + OH = C3H7 + HCO	0.168E+11	-0.339E+03
78	C4H7 + H = C2H6 + C2H2	0.278E+11	0.679E+01
79	C4H7 + O = C3H7 + CO	0.168E+11	-0.339E+03
80	C4H7 + O = C2H5O + C2H2	0.227E+12	-0.105E+04
81	CH3 + C3H7 = C4H8 + H2	0.268E+10	0.188E+03
82	C2H5 + C2H5 = C4H8 + H2	0.449E+09	0.190E+03
83	C4H8 + H + H = CH3 + C3H7	0.134E+07	-0.467E+04
84	C4H8 + H + H = C2H5 + C2H5	0.802E+07	-0.489E+04
followed by the oxidation mechanism of C1-C3 hydrocarbons			

2. Mechanism Validation

The new reaction mechanism was validated against experimental data on C_4H_{10} self-ignition and oxidation available in literature.

The equations describing self-ignition and oxidation of a homogeneous mixture at constant-volume conditions are written in the form [9]:

$$\frac{dn_j}{dt} = \sum w_{ij} \tag{1}$$

$$\tilde{n}c_v \frac{dT}{dt} = \sum \Delta H_{ij} w_{ij} + kF(T - T_w)/V \tag{2}$$

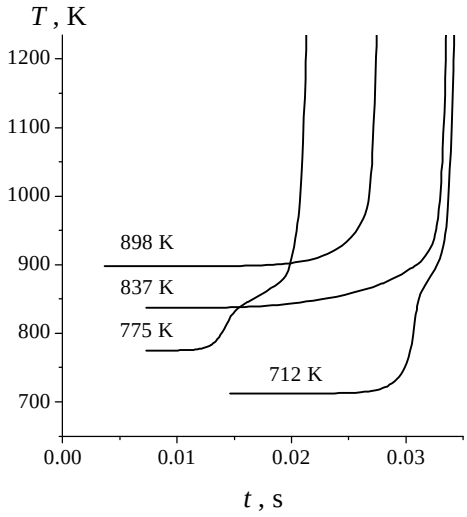

Figure 1: Predicted temperature histories during self-ignition of 3.11%*n*-butane – air mixture at P_0 = 10.22 bar.

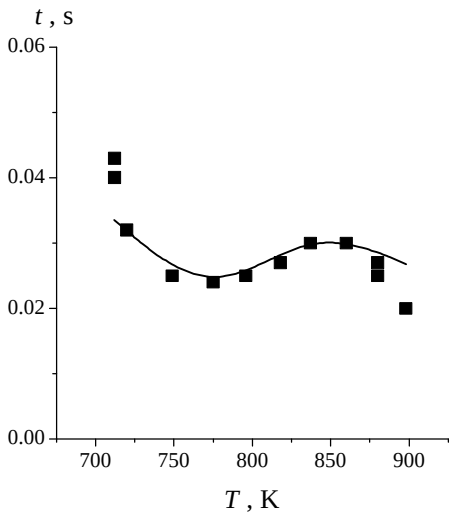

Figure 2: Comparison of predicted (curve) and measured (symbols, [10]) ignition delay times for 3.11%C_4H_{10}–20.25%O_2–N_2–Ar mixture at P_0= 9.39–11.85 bar.

Here, n_j is the *j*th species molar concentration, *t* is time, r is the density, c_v is the specific heat at constant volume, w_{ij} and ΔH_{ij} are the rate and heat effect of the *i*th elementary reaction with participation of the *j*th species, k is the heat transfer coefficient to the reactor walls, *F* and *V* are the reactor surface area and volume, and T_w is the wall temperature. The first term in the right-hand side of Eq. (2) corresponds to heat release due to chemical reactions and the second term corresponds to the heat loss to the reactor walls. The density was calculated using the ideal gas equation of state $r = P/RT$, where *P* is the pressure.

The initial conditions for Eqs. (1) and (2) are:

$$n(0) = n_{j0} \text{ and } T(0) = T_0 \qquad (3)$$

2.1 Experiments of Minetti and Sochet [10]

When modeling oxidation or self-ignition phenomena at relatively high pressures and low temperatures, heterogeneous reactions at the reactor walls and heat transfer to the walls can be neglected. Figure 1 shows typical time histories of temperature at self-ignition of *n*-butane – air mixture. At low temperatures, a two-stage self-ignition is clearly seen: the hot explosion is preceded by the cool flame. This phenomenon results in the Negative Temperature Coefficient (NTC) of the reaction rate constant and longer ignition delay times at a higher temperature (Fig. 2).

At certain conditions, a multistage rather than two-stage self-ignition occurs, which is typical for hydrocarbon oxidation [3]. As an example, Figs. 3*a* to 3*d* show the predicted results for self-ignition of 10%C_4H_{10} – air mixture at T_0 = 712 K and P_0 = 9.4 bar. One can clearly see the inflection points at the temperature curves and at the time histories of stable and intermediate species concentrations (hydroxyl), which correspond to multistage self-ignition with the onset of cool and blue flame, as well as hot explosion. Cool flames arise due to decomposition of alkyl hydroperoxides, namely butyl hydroperoxide, $C_4H_{10}O_2H$. At its decomposition, chain branching occurs and the concentration of hydroxyl increases drastically leading to the corresponding increase in the oxidation rate of C_4H_{10}. After consumption of the accumulated butyl hydroperoxide, the reaction rate of *n*-butane oxidation decreases. At this stage, hydrogen

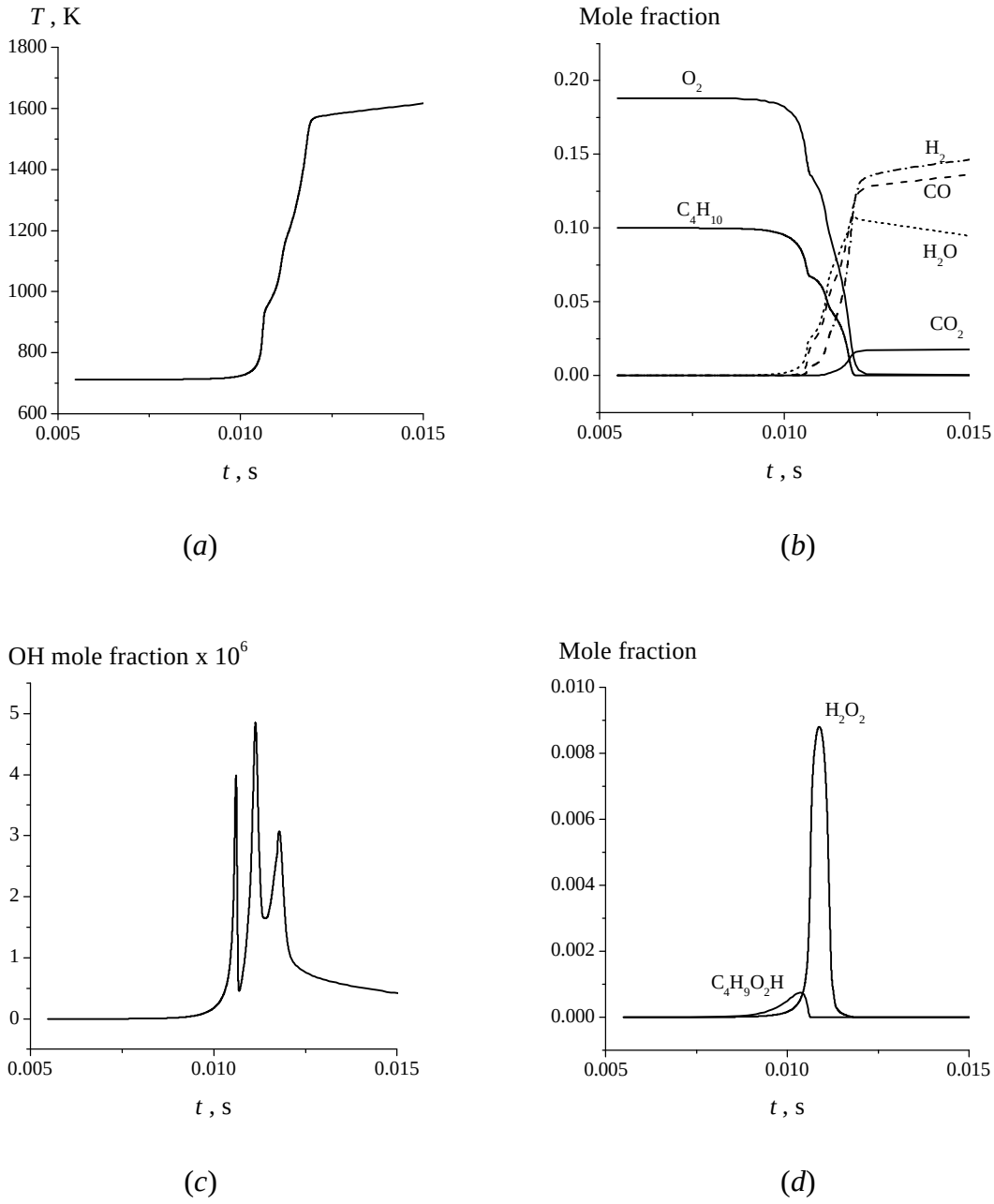

Figure 3: Predicted time histories of temperature (*a*), stable species mole fractions (*b*), hydroxyl mole fraction (*c*), and mole fractions of butyl hydroperoxide and hydrogen peroxide (*d*) during self-ignition of 10%*n*-butane – air mixture at P_0 = 9.4 bar and T_0 = 712 K.

peroxide, H_2O_2, starts accumulating. Subsequent decomposition of hydrogen peroxide, also leading to chain branching, manifests itself in the second maximum of the hydroxyl concentration and in the incipience of blue flame. The subsequent growing rate of chain branching is due to classical reaction of H atom with O_2, which causes the third maximum of hydroxyl concentration corresponding to hot explosion.

2.2 Experiments of Dechaux et al. [11]

At low pressures and temperatures, one has to take into account heterogeneous reactions at the reactor walls and heat transfer to the walls [9]. Heterogeneous oxidation reactions at the reactor walls are poorly studied and therefore will not be considered here, except for the diffusion controlled reaction of butyl hydroperoxide and hydrogen peroxide decomposition with the

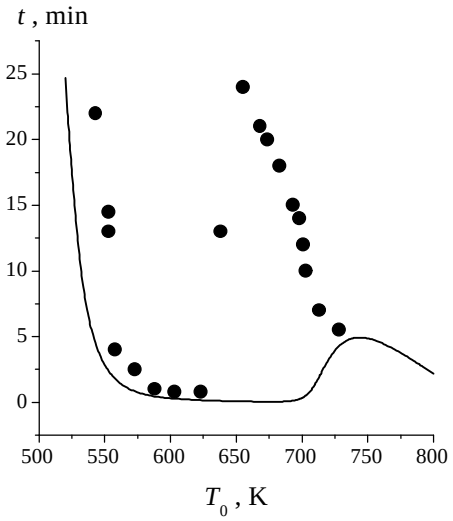

Figure 4: Comparison of predicted (curve) and measured (symbols, [11]) delay times of reaction onset in 20%*n*-butane – 80%O_2 mixture at P_0 = 52 mm Hg.

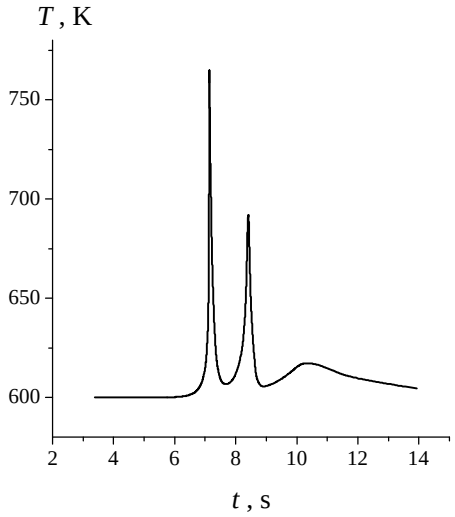

Figure 5: Predicted temperature history during oxidation of 20%*n*-butane – 80%O_2 mixture at T_0 = 600 K and P_0 =52 mm Hg.

formation of stable products. The heat transfer to the wall in experiments [11] can be readily estimated: $\kappa F/V \approx 13.7–35.2$ cal/l/s. Figure 4 shows the comparison of predicted and measured delay times of reaction onset at different temperatures and a pressure of P_0 = 52 mm Hg. In the experiments of [11], one can clearly see the NTC region in the temperature range T_0 = 625–660 K. The predicted NTC region is considerably less pronounced and is shifted to the temperature range T_0 = 700–730 K. To the left of the NTC region, cool flame is observed in both experiments and calculations. To the right of the NTC region, slow oxidation of *n*-butane takes place with the poorly pronounced delay time of reaction onset. The predicted temperature history at T_0 = 600 K and P_0 = 52 mm Hg is shown in Fig. 5. Three successive cool flames are evident in Fig. 5. At higher temperatures, such cool flames disappear. In general, despite a considerable quantitative disagreement, probably due to incorrect neglecting of heterogeneous reactions at the reactor wall at low pressure, the qualitative agreement with the measurements is worth noting.

2.3 Experiments of Burcat et al. [12]

Figure 6 compares predicted and measured self-ignition delay times of 2.5%C_4H_{10} – 20%O_2 – Ar mixture at P_0 = 9.19–10.58 bar and T_0 = 1230–1370 K. A good quantitative agreement of the results is obtained.

2.4 Experiments on Flame Propagation [13-17]

The oxidation mechanism of *n*-butane was used to calculate the laminar burning velocity, u_n, in the *n*-butane–air mixture at normal conditions (P_0 = 1 bar and T_0= 293 K) using the code described in [18]. For the stoichiometric *n*-butane–air mixture with the equivalence ratio $\Phi = 1.0$ the predicted laminar burning velocity is u_n=34.8 cm/s, which corresponds well with the experimental value varying from 33.1 to 44.5 cm/s (Table 3).

3. Discussion and Concluding Remarks

The new detailed reaction mechanism of *n*-butane oxidation has been developed and validated against available experimental data. The availability of such a mechanism is important for

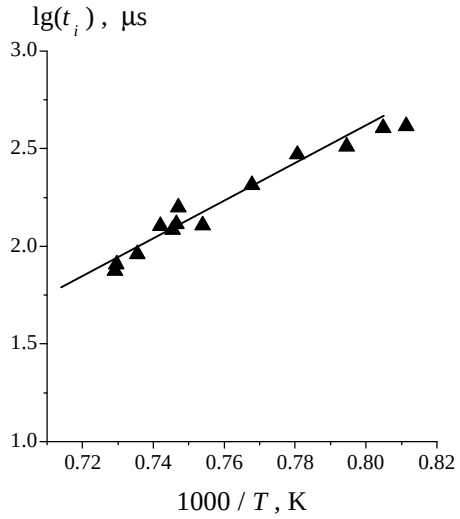

Figure 6: Comparison of predicted (curve) and measured (symbols, [12]) self-ignition delay times of 2.5%C_4H_{10} – 20%O_2 – Ar mixture at P_0 = 9.19–10.58 bar and T_0 = 1230–1370 K.

Table 3: Laminar burning velocity in the stoichiometric n-butane – air mixture ($\Phi = 1.0$) at P_0 = 1 bar and T_0= 293 K.

u_n, cm/s	Reference
33.8 at $\Phi = 0.93$	[13]
34.1 and 33.1 at $\Phi = 1.17$	[13]
35.2	[14]
44.5	[15]
41.4	[16]
37.1	[17]

understanding fundamental reasons of accidental explosions occurring, e.g., at catalytic oxidation of *n*-butane for production of maleic anhydride, $C_4H_2O_3$, and other compounds of industrial interest. Large-scale industrial reactors operating at elevated pressures (higher than 3 bar) and temperatures (550–650 K) are at risk of working mixture self-ignition, in particular in view of long residence times involved.

Comparison of calculations with available experimental data indicates that the new detailed reaction mechanism of *n*-butane oxidation developed in this study provides satisfactory predictions of low-temperature and high-temperature self-ignition delays and laminar burning velocities at normal and elevated pressures. This means that the new mechanism is capable of predicting the conditions for the onset of accidental explosions in industrial reactors using *n*-butane as a reactant. Besides, the principle of mechanism construction and the underlying assumptions were proved to be reasonable and could be used for the development of oxidation mechanisms of higher *n*-alkane hydrocarbons.

Acknowledgments

This work was supported by the Russian – Dutch Research Cooperation project No. NWO 046.016.012, and Russian Foundation for Basic Research projects 05-08-18200a, 05-08-50115a, and 05-08-33411a.

References

1. Chevalier, C., Louessard, P., Muller, U.C., & Warnatz, J. (1990) Joint Meeting Sov. Ital. Sections Comb. Inst., The Comb. Inst., Pisa. 5.
2. Buda, F., Bounaceur, R., et al. (2005) *Comb. Flame, 142*. 170.
3. Sokolik, A. S. (1960) Self-ignition, flame, and detonation in gases. Moscow: USSR Acad. Sci. Publ.
4. Lewis, B., & Elbe, G. (1987) Combustion, flames and explosions of gases. Orlando: Acad. Press.
5. Warnatz, J. (1983) *Comb. Sci &Techn., 34*. 177.
6. Ranzi, E., Faravelli, T., et al. (1994) *Comb. Sci & Techn., 100*. 299.
7. Basevich, V. Ya., Vedeneev, V. I., Frolov, S. M., & Romanovich, L. B. (2005) *Rus. J. Chemical Physics, 24*(2). 105.
8. Semenov, N. N. (1958) Some problems in chemical kinetics and reactivity. Moscow: USSR Acad. Sci. Publ.
9. Kondratiev, V. N., & Nikitin, E. E. (1974) Kinetics and mechanism of gas-phase reactions. Moscow: Nauka Publ.
10. Minetti, R., & Sochet, R. (1994) *Comb. Flame, 96.* 201.
11. Dechaux, J. C., Flament, J. L., & Lucquin, M. (1971) *Comb. Flame, 17.* 205.
12. Burcat, A., Scheller, K., & Lifshitz, A. (1971) *Comb. Flame, 16.* 29.
13. Gerstein, M., Levin, O., & Wong, E. L. (1951) *J. Amer. Chem. Soc., 73.* 418.
14. Gibbs, G. I., & Calcote, H. F. J. (1959) *Chem. Eng. Data, 4*. 226.
15. Karpov, V. P., & Sokolik, A. S. (1961) *Doklady USSR Acad. Sci., 138*. 874.
16. Hirasawa, T., Sung, C. J., et al. (2002) Proc. 29 Symp. (Intern.) on Comb. The Comb. Inst. 1427.
17. Bosschaart, K. J., & de Goey, L. P. H. (2004) *Comb. Flame, 136*. 261.
18. Belyaev, A. A., & Posvianskii, V. S. (1985) In: *Algorithms and Codes*. Information Bulletin of USSR Foundation of Algorithms and Codes, 3. 35.